

Complete substitution of Fe²⁺ by Mg in Fe₄O₅: The crystal structure of the Mg₂Fe₂O₅ end-member

TIZIANA BOFFA BALLARAN^{1,*}, LAURA UENVER-THIELE² AND ALAN B. WOODLAND²

¹Bayerisches Geoinstitut, Universität Bayreuth, D-95440 Bayreuth, Germany

²Institut für Geowissenschaften, Goethe-Universität Frankfurt, Altenhöferallee 1, D-60438 Frankfurt am Main, Germany

ABSTRACT

The crystal structure of a novel Mg₂Fe₂O₅ oxide synthesized at 15 GPa and 1550 °C has been determined by means of single-crystal X-ray diffraction. This compound is isostructural with Fe₄O₅ and can be considered as the other end-member of a solid solution between these two oxides involving the substitution of Fe²⁺ for Mg. The resulting unit-cell lattice parameters $a = 2.8889(4)$, $b = 9.7282(4)$, and $c = 12.5523(7)$ Å are smaller than those of Fe₄O₅. Mg and Fe³⁺ cations are found to be disordered among the three crystallographic sites of the Mg₂Fe₂O₅ structure, although preference of Mg for the trigonal prism coordination (M3) is observed. Substitution of Mg into the Fe₄O₅ structure reduces the octahedral distortion of both the M1 and M2 sites. Like Mg, Cr has recently been found to substitute into Fe₄O₅, so that Fe³⁺/ΣFe can vary from 0 to 1.0 in the Mg-Cr-Fe oxides system. Substitution of both Mg and Cr in Fe₄O₅ also makes this phase more relevant for bulk compositions expected in the Earth's transition zone and deep upper mantle. M₄O₅ phases having the CaFe₃O₅-type structure, therefore, need to be considered as a new addition to the phase relations of several simple oxide systems at pressure and temperature conditions at which the spinel-structured phases become unstable.

Keywords: Mg₂Fe₂O₅, Fe₄O₅, transition zone, high-pressure, crystal structure

INTRODUCTION

Fe₄O₅ is a novel oxide recently observed as a breakdown product of siderite (Lavina et al. 2011) or magnetite (Woodland et al. 2012). The stability field of Fe₄O₅ has been studied experimentally and it is known to extend to pressures of at least 24 GPa. The relevance of this phase for the Earth's mantle was described by Woodland et al. (2013), who demonstrated that Mg and Cr may substitute for Fe²⁺ and Fe³⁺, respectively. The structure of the Fe₄O₅ end-member has been determined mainly by powder diffraction and DFT calculations (Lavina et al. 2011; Trots et al. 2012; Guignard and Crichton 2014), as the number of observed structure factors from the single-crystal experiment reported in Lavina et al. (2011) was extremely small (20 independent reflections). The data collected so far are consistent with a *Cmcm* space group and a structure similar to that of Sr₂Tl₂O₅ and CaFe₃O₅, consisting of layers of edge-sharing FeO₆ octahedra and layers of trigonal prisms alternating along the *c*-axis. Some discrepancies are apparent in the size and distortion of the FeO₆ octahedra among the room-pressure determinations, most likely due to the difficulty in accurately determining the oxygen positions from X-ray powder diffraction patterns (Trots et al. 2012; Guignard and Crichton 2014). In spite of these distortions, the CaFe₃O₅-type structure appears more flexible than might be expected from the edge- or face-sharing nature of its polyhedral units as it can accommodate a large variety of cations.

It has been observed that not only magnetite, but also chromite (FeCr₂O₄) dissociates into Fe₂Cr₂O₅ and Cr₂O₃ at high pressure (Ishii et al. 2014). However, Ishii et al. (2014) report that Fe₂Cr₂O₅ is isostructural with Mg₂Al₂O₅ (Enomoto et al.

2009), having space group *Pbam*. This is quite puzzling given that samples belonging to the Fe-Cr solid solution with up to 50% Fe₂Cr₂O₅ component (Woodland et al. 2013) appear instead to crystallize in the *Cmcm* space group. The major difference between the *Cmcm* Fe₄O₅ and the *Pbam* Fe₂Cr₂O₅ structures lies in the stacking of the octahedral units that form long chains surrounding the trigonal prisms in the latter compound. Note, however, that the Fe₂Cr₂O₅ structure was also solved using X-ray powder diffraction patterns (Ishii et al. 2014).

Like Cr, Mg can substitute into the Fe₄O₅ structure (Woodland et al. 2013). However, whether complete Mg substitution in Fe₄O₅ is possible and whether such a substitution gives rise to a change in symmetry is still unknown.

Here, we report the synthesis and crystal structure of Mg₂Fe₂O₅, based upon X-ray single-crystal diffraction. Single-crystal structural data allow not only to determine accurately the space group of this material as well as the oxygen positions and the displacement parameters of all atoms present in the structure, but also to provide important constraints on the cation occupancies of the distinct crystallographic sites in this phase.

EXPERIMENTAL METHODS

Starting material

The starting material was a stoichiometric mixture of MgO and pre-synthesized MgFe₂O₄. The MgFe₂O₄ was synthesized following a procedure modified from that outlined in Levy et al. (2004) using sintered MgO and Fe₂O₃. A stoichiometric mixture of MgO and Fe₂O₃ was pressed into pellets and held at 1000 °C for 40 h in a muffle furnace (at 1 atm). The pellets were then reground, repressed into pellets and sintered at 1000 °C for 24 h. In a final step, the furnace temperature was lowered progressively to 950 °C and held for 24 h, followed by further sintering at 900 °C for another 24 h. The sample was then removed from the furnace and allowed to cool to room temperature. The resulting material was a fine light red brown powder. Analysis by X-ray powder diffraction using a Philips X'Pert PRO diffractometer with monochromatic CoKα₁ radiation and an internal Si standard revealed only

* E-mail: tiziana.boffa-ballaran@uni-bayreuth.de

a small trace of hematite along with magnesioferrite having a unit-cell parameter of $a = 8.3875(1)$ Å. This value is consistent with stoichiometric magnesioferrite with a degree of inversion $x = 0.84$ (O'Neill et al. 1992).

Sample synthesis and characterization

The synthesis of $\text{Mg}_2\text{Fe}_2\text{O}_5$ was carried out at 15 GPa and ~1550 °C in a 1000-t multi-anvil press at the Bayerisches Geoinstitut, Universität Bayreuth, Germany. The pressure calibration of the multi-anvil apparatus was reported by Keppler and Frost (2005). The experiment was performed using a Cr_2O_3 -doped MgO pressure assembly with a 10 mm edge length and WC cubes with 5 mm truncations. The starting material was packed into a Pt-foil capsule along with a small amount of PtO_2 at the bottom and the top to avoid reduction during the experiment. The high oxygen fugacity produced by PtO_2 in the experiment means that Fe loss to the Pt capsule is negligible. Heating was achieved with a LaCrO₃ furnace and the temperature was monitored by a $\text{W}_3/\text{Re}_{97}$ – $\text{W}_{25}/\text{Re}_{75}$ thermocouple with the electromotive force (emf) uncorrected for pressure. The heating duration at high-pressure was 2.75 h. The run product (experiment H3975) consisted of large crystals of prismatic shape and dark color. The composition of these crystals was analyzed on a five-spectrometer JEOL JXA-8900 superprobe at the Institut für Geowissenschaften in Frankfurt am Main, Germany. Pure oxides MgO and Fe_2O_3 were used as primary standards and a ZAF algorithm was used for matrix correction. Measurements were performed on a polished grain mount in wavelength-dispersive mode with a 15 kV accelerating voltage, a beam current of 20 nA and a focused beam. Integration times were 40 s on the peak and background. Microprobe analysis yielded a composition of 33.49(17) wt% MgO and 67.10(1.05) wt% Fe_2O_3 (average of 5 points), corresponding to a stoichiometry of $\text{Mg}_{1.99(2)}\text{Fe}_{2.01(2)}\text{O}_5$. Thus, within analytical uncertainties, our sample has an ideal $\text{Mg}_2\text{Fe}_2\text{O}_5$ composition.

X-ray single-crystal diffraction

The single crystal (~75 × 60 × 35 μm^3) used for the intensity collection by means of X-ray diffraction was selected on the basis of its relatively sharp diffraction profiles. Typical half-widths of different reflections were between 0.095 and 0.130° in ω . Intensity data were collected from the single crystal mounted on a glass fiber at ambient conditions using an Xcalibur diffractometer with MoK α radiation operated at 50 kV and 40 mA, equipped with a CCD detector and a graphite monochromator. Omega scans were chosen to obtain a large redundancy of the reciprocal sphere up to $2\theta_{\text{max}} = 72^\circ$. The exposure time was 20 s/frame. Lorentz and polarization factors as well as an analytical absorption correction based on the crystal shape were taken into account for the correction of the reflection intensities using the CrysAlis package (Oxford Diffraction 2006). No indication of twins was observed in the measured reflections. The observed reflections conditions were consistent with the $Cmcm$ space group; therefore, structure refinements based on F^2 were performed using the starting parameters of Fe_4O_5 from Trots et al. (2012) and the SHELX97 program package (Sheldrick 2008) in the WinGX System (Farrugia 1999). The scattering curves for neutral species (Ibers and Hamilton 1974) were used for Mg, Fe, and O, and all atoms were refined anisotropically. Mg and Fe occupancies were refined at each site with the sum of their occupancy factors constrained to unit. Data collection and refinement details are reported in Table 1 whereas fractional atomic coordinates, displacement parameters, and polyhedral bond lengths are given in Tables 2 and 3, respectively. (CIF¹ available.)

RESULTS AND DISCUSSION

The refined crystal structure of $\text{Mg}_2\text{Fe}_2\text{O}_5$ indicates that this compound is isostructural with CaFe_3O_5 (Evrard et al. 1980) with layers of edge-sharing octahedra (M1 and M2 sites) alternating

with layers of triangular prisms along the c -axis (M3 site) (Fig. 1). Refinement of the Mg and Fe occupancies at the M1, M2, and M3 sites for the crystal investigated in this study reveals a chemical composition, within analytical uncertainties, of $\text{Mg}_2\text{Fe}_2\text{O}_5$. This is in excellent agreement with microprobe analysis of grains from the same run product (H3975) from which the crystal was extracted. Thus, our sample represents the Mg end-member of Fe_4O_5 and suggests that there is complete solid solution involving cation substitution of Fe^{2+} and Mg^{2+} as proposed by Woodland et al. (2013). No change in symmetry is apparent across the join, in contrast to what seems to occur in the Fe-Cr system (Ishii et al. 2014; Woodland et al. 2013).

In Fe_4O_5 , all structural sites are occupied by Fe. Although an accurate determination of the site distributions of Fe^{2+} and Fe^{3+} among the different structural sites of this compound remains undetermined, as a first approximation one could expect Fe^{2+} to occupy the M1 and Fe^{3+} the M2 site of the structure as described by Evrard et al. (1980) for CaFe_3O_5 (in the case of Fe_4O_5 , Fe^{2+} occupies also the triangular prism, M3). However, such a description of the cation distribution in Fe_4O_5 is likely too simple, given that even for CaFe_3O_5 thermally activated electron transfer has been observed already at room temperature (Gerardin et al. 1985). Since the M1-M2 distance between the Fe cations in Fe_4O_5 ranges between 2.945 and 2.991 Å (Trots et al. 2012; Guignard and Crichton 2014), i.e., is even smaller than that reported for CaFe_3O_5 , electron transfer can also be expected for Fe_4O_5 . This charge transfer can give rise to a complex and dynamic site distribution of Fe^{2+} and Fe^{3+} on a local scale. A complex cation distribution is also observed in $\text{Mg}_2\text{Fe}_2\text{O}_5$ with Mg substituting at all sites (Table 2), although there is a slight preference for this cation to occupy the M3 and M2 sites. In

¹ Deposit item AM-15-25138, CIF. Deposit items are stored on the MSA web site and available via the American Mineralogist Table of Contents. Find the article in the table of contents at GSW (ammin.geoscienceworld.org) or MSA (www.minsocam.org), and then click on the deposit link.

TABLE 1. Unit-cell lattice parameters and structural refinement details for $\text{Mg}_2\text{Fe}_2\text{O}_5$

Max. 2θ	72.53°		
Measured reflections	3720	Absorption coefficient	8.47 mm ⁻¹
Unique reflections	493	Space group	$Cmcm$
$F_o > 4\sigma(F_o)$	472	Z	4
R_{int}	3.86	Unit-cell parameters	
R_w for $F_o > 4\sigma(F_o)$	3.85		
R_{all}	4.09		
$wR2$	9.47		
Goof	1.126		
No. parameters	37		
F(000)	464	a (Å)	2.8889(4)
		b (Å)	9.7282(4)
		c (Å)	12.5523(7)
		V (Å ³)	352.77(5)

Note: Standard deviations are in parentheses.

TABLE 2. Atomic positions and displacement parameters of $\text{Mg}_2\text{Fe}_2\text{O}_5$ (standard deviations are in parentheses)

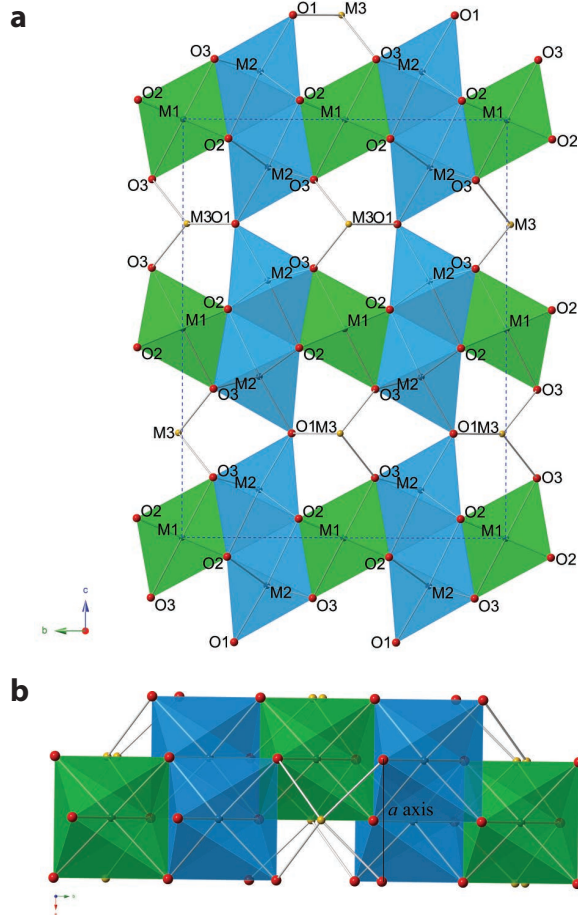
	M1	M2	M3	O1	O2	O3
Wyckoff position	4a	8f	4c	4c	8f	8f
x	0.0	0.0	0.0	0.0	0.0	0.0
y	0.0	0.26240(5)	0.51220(13)	0.1621(3)	0.3603(2)	0.0958(2)
z	0.0	0.11458(4)	0.25	0.25	0.5458(2)	0.6440(2)
Mg occupancy	0.5327(8)	0.2959(17)	0.8589(8)			
Fe occupancy	0.4673(8)	0.7041(17)	0.1411(8)			
U_{11}	0.0101(4)	0.0101(4)	0.0108(6)	0.0139(12)	0.0110(8)	0.0156(9)
U_{22}	0.0045(3)	0.0060(2)	0.0097(5)	0.0091(11)	0.0081(8)	0.0074(8)
U_{33}	0.0082(4)	0.0103(3)	0.0258(8)	0.0117(12)	0.0171(10)	0.0114(9)
U_{23}	0.0010(2)	-0.0002(2)	0.0	0.0	0.0033(7)	0.0003(6)
U_{eq}	0.0076(2)	0.0088(2)	0.0154(3)	0.0116(5)	0.0121(4)	0.0114(4)

TABLE 3. Bond distances (Å), octahedral volumes (Å³), and angles (°) of $\text{Mg}_2\text{Fe}_2\text{O}_5$, Fe_4O_5 at room pressure and Fe_4O_5 at 10 GPa (Lavina et al. 2011)

	$\text{Mg}_2\text{Fe}_2\text{O}_5$	Fe_4O_5^a	Fe_4O_5^b	Fe_4O_5 at 10 GPa ^c
M1				
Fe(Mg)-O3(x2)	2.034(2)	2.021	1.993	1.941
Fe(Mg)-O2(x4)	2.0645(14)	2.122	2.090	2.028
<Fe(Mg)-O>	2.054(2)	2.088	2.041	1.999
V_{M1}	11.526(18)	12.05	11.51	10.6
*OAV _{M1}	0.0032	0.0077	0.0112	0.0008
O2-O2(x2)	2.889(2)	2.893	2.896	2.843
O2-O2(x2)	2.951(2)	3.105	3.020	2.893
O2-O3(x4)	2.818(2)	2.827	2.742	2.807
O2-O3(x4)	2.976(2)	3.030	3.032	2.808
O2-M1-O2(x2)	88.78(7)	85.95	87.6	89.0
O2-M1-O2(x2)	91.21(7)	94.05	92.4	91.0
O2-M1-O3(x4)	86.89(7)	86.04	84.2	90.0
O2-M1-O3(x4)	93.11(7)	93.96	95.6	90.0
O2-M1-O2(x2)	180	180	180	180
O3-M1-O3	180	180	180	180
M2				
Fe(Mg)-O1	1.9599(16)	1.919	1.878	1.960
Fe(Mg)-O3(x2)	2.0314(14)	2.026	2.088	2.090
Fe(Mg)-O2(x2)	2.0637(14)	2.034	2.084	2.032
Fe(Mg)-O2	2.227(2)	2.270	2.135	2.241
<Fe(Mg)-O>	2.0628	2.052	2.033	2.074
V_{M2}	11.489(17)	11.21	11.30	11.7
*OAV _{M2}	0.0053	0.0078	0.0137	0.0095
O2-O3(x2)	2.854(2)	2.778	2.915	2.947
O2-O2	2.889(2)	2.893	2.896	2.843
O3-O3	2.889(2)	2.893	2.896	2.843
O2-O3(x2)	2.819(2)	2.827	2.742	2.808
O2-O2(x2)	2.830(2)	2.774	2.675	2.917
O1-O2(x2)	2.951(2)	2.932	3.056	2.848
O1-O3(x2)	3.066(2)	3.070	3.038	3.157
O2-M2-O3(x2)	88.37(8)	86.35	88.7	91.2
O2-M2-O2	88.84(8)	91.12	86.6	88.8
O3-M2-O3	90.64(8)	90.65	89.5	85.7
O2-M2-O3(x2)	82.75(7)	81.94	82.1	80.7
O2-M2-O2(x2)	82.48(7)	80.21	78.5	85.9
O2-M2-O1(x2)	94.30(8)	95.97	99.1	91.0
O3-M2-O1(x2)	100.39(8)	101.87	100.1	102.4
O2-M2-O3(x2)	165.21(10)	162.41	160.6	166.6
O2-M2-O1	175.48(9)	174.49	176.7	174.49
M2-O1-M2	120.287	121.16	125.0	118.3
M3				
Fe(Mg)-O1(x2)	2.053(2)	2.107	2.203	2.056
Fe(Mg)-O3(x4)	2.2269(17)	2.239	2.200	2.123
Fe(Mg)-O2(x2)	2.848(2)	2.883	3.001	2.763
<Fe(Mg)-O> ₆	2.169	2.195	2.201	2.101
<Fe(Mg)-O>	2.339	2.367	2.401	2.266

Note: *OAV = octahedral angle variance (Robinson et al. 1971). ^aTrots et al. (2012). ^bGuignard and Crichton (2014). ^cLavina et al. (2011).

particular, the M3 site is almost fully occupied by Mg (85%), causing a reduction in the a -parameter, which in this particular structure is equal to the height of the triangular prism expressed as O3-O3 (or O1-O1) distances (Fig. 1b) (Evrard et al. 1980). This particular distance correlates non-linearly with the size of the cation occupying the M3 site (Fig. 2), suggesting that for smaller cations such as Fe^{2+} and Mg, O-O repulsion starts to play a role in determining how close the anions can approach each other. The fact that no significant correlation between the a -parameter and Mg content (Fig. 3) is observed for small amounts of Mg substitution in Fe_4O_5 (Woodland et al. 2013) supports a random distribution of Mg and Fe^{2+} among all sites in such compositions. Clearly changes in the O3-O3 distance can be observed at the long range scale of the X-ray measurements only once a significant amount of Mg is present at the M3 site, resulting in shorter M3-O bond distances. This can occur only for Mg-rich samples, given the random distribution of Mg/Fe^{2+} among the

**FIGURE 1.** Crystal structure of $\text{Mg}_2\text{Fe}_2\text{O}_5$ projected (a) down the a axis and (b) down the c axis.

structural sites. Unfortunately, it is impossible at present to assess the value of the critical occupancy of Mg at the M3 site for which a decrease of the a -parameter can be observed, since the site distributions in the samples of Woodland et al. (2013) are not known. It is clear, however, that the degree of Mg/Fe^{2+} disorder must be quite large even in samples containing up to 0.5 Mg atoms per formula unit (apfu), as no significant change in the a -parameter with respect to the value for the Fe_4O_5 end-member is observed (Fig. 3).

The Mg-poor samples described by Woodland et al. (2013) were all synthesized at much lower temperature (1100 °C) than that used for the synthesis of $\text{Mg}_2\text{Fe}_2\text{O}_5$ in this study (~1550 °C). Considering that higher temperatures usually favor higher degrees of cation disorder (as observed in various spinels, e.g., O'Neill and Navrotsky 1983), the preference of Mg for the M3 site observed in $\text{Mg}_2\text{Fe}_2\text{O}_5$ must be of a crystal-chemical nature rather than being only due to thermal effects or to quenching of the synthesis experiments.

The major effect of Mg substitution is to reduce the octahedral distortion of both the M1 and M2 sites (Table 3) with respect to the Fe_4O_5 end-member, as shown by the major decrease in octahedral angle variance (OAV) (Robinson et al. 1971). This

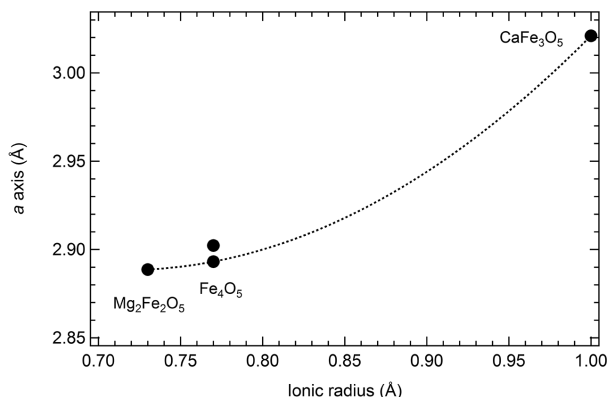


FIGURE 2. Correlation between the a -parameter (i.e., height of the triangular prism M3) and the size of the cation occupying the M3 site in the CaFe_3O_5 -type structures; Ca in CaFe_3O_5 , Fe^{3+} in Fe_4O_5 and Mg in $\text{Mg}_2\text{Fe}_2\text{O}_5$. Note that for $\text{Mg}_2\text{Fe}_2\text{O}_5$ the cation size has been calculated taking into account the site occupancy derived from the structural refinements (Table 2). The values of the a -parameter are taken from Trots et al. (2012) for Fe_4O_5 and from Evrard et al. (1980) for CaFe_3O_5 .

effect is particularly apparent for the M1 site, which is half occupied by Mg. The individual bond distances become much more similar, giving rise to a less flattened octahedron compared to Fe_4O_5 (Table 3). Moreover, the major decrease of the M1-O2 bond distance in $\text{Mg}_2\text{Fe}_2\text{O}_5$ with respect to the Fe end-member may have a primary role in the shortening of the unit cell b axis (Woodland et al. 2013). The M2 site is better described as rectangular pyramid (Evrard et al. 1980) since one of the bond lengths (M2-O2) of the octahedral coordination is much longer than the other five. In spite of the smaller degree of Mg substitution in this site (less than 30%, Table 2), a major decrease of the M2-O2 bond length can be observed and, therefore, the M2 coordination in the $\text{Mg}_2\text{Fe}_2\text{O}_5$ end-member becomes more octahedron-like.

Compression of any material, especially at mantle pressures is unlikely to occur without octahedral deformation. However, we can still expect that tilting between octahedra will have a much lower energy and should, therefore, play a major role as compression mechanism at least at relatively low pressures. In the $\text{Mg}_2\text{Fe}_2\text{O}_5$ - Fe_4O_5 system the only tilting mechanism possible is represented by the M2-O1-M2 angle (Table 3, Fig. 1a) whose value indeed appears to decrease both with Mg substitution and with pressure (Table 3). The question arises of whether this angle also may play a role on determining the stability field of this compound, since the O3-O3 distance of neighboring M2 octahedra in $\text{Mg}_2\text{Fe}_2\text{O}_5$ [2.660(2) Å] is already shorter than the O-O distances defining the coordination of the M1 and M2 sites (Table 3). Thus, anion-anion repulsions may hinder the tilting at high pressures resulting either in a compression mechanism based exclusively on octahedral distortion and/or a phase transformation.

IMPLICATIONS

We have demonstrated that a Mg-bearing end-member, $\text{Mg}_2\text{Fe}_2\text{O}_5$, isostructural with Fe_4O_5 , is stable at high pressure and temperature. This, along with the data of Woodland et al. (2013), provides further evidence that complete Fe^{2+} -Mg solid solution is likely between Fe_4O_5 and $\text{Mg}_2\text{Fe}_2\text{O}_5$. The experimental deter-

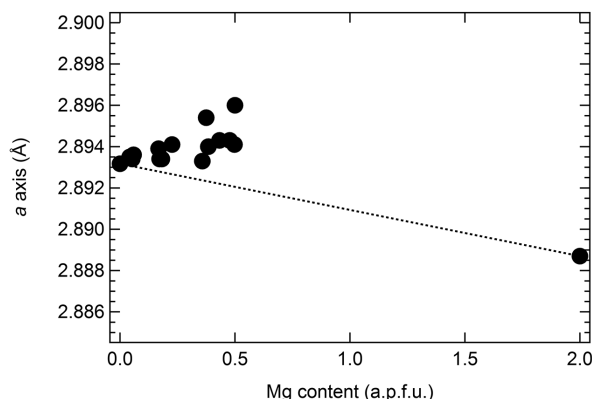


FIGURE 3. Variation of the a lattice parameter as a function of Mg content in $\text{Mg}_2\text{Fe}_2\text{O}_5$ and $(\text{Mg,Fe})_2\text{Fe}_2\text{O}_5$ solid solution reported by Woodland et al. (2013). Error bars are smaller than the symbols.

mination of the detailed phase relations involving $\text{Mg}_2\text{Fe}_2\text{O}_5$ is currently under study (Uenver-Thiele et al. 2014). It is important to note that not only does Fe_4O_5 form from the breakdown of magnetite at a pressure of ~ 10 GPa (Woodland et al. 2012), but MgFe_2O_4 also breaks down in an analogous fashion to the assemblage $\text{Mg}_2\text{Fe}_2\text{O}_5 + \text{Fe}_2\text{O}_3$ under similar pressure-temperature conditions (Uenver-Thiele et al. 2014).

Recent studies by Woodland et al. (2013) and Ishii et al. (2014) indicate that Cr can also substitute for Fe^{3+} in Fe_4O_5 and that a phase with $\text{Fe}_2\text{Cr}_2\text{O}_5$ stoichiometry is stable at least at pressures of 12–16 GPa and 800–1600 °C. However, the substitution of Cr appears different in detail with respect to the Mg substitution, given that $\text{Fe}_2\text{Cr}_2\text{O}_5$ crystallizes with a different space group. Although the $\text{Fe}_2\text{Cr}_2\text{O}_5$ structural analysis still needs to be confirmed by single-crystal X-ray data, a possible explanation of such a difference may reside in the different Jahn-Teller distortions in the two compounds, since in $\text{Fe}_2\text{Cr}_2\text{O}_5$ only Cr^{3+} is present while in $\text{Mg}_2\text{Fe}_2\text{O}_5$ the transition cation is exclusively Fe^{3+} . Transformation from the $Cmcm$ to the $Pbam$ phase, however, appears to occur only at very high Cr compositions, given that samples containing up to 0.92 atoms per formula unit of Cr appear to have still the Fe_4O_5 structure (Woodland et al. 2013).

Potential substitution of both Mg and Cr in Fe_4O_5 not only makes this phase more relevant for bulk compositions expected in the Earth's transition zone, it also means that through cation substitution the $\text{Fe}^{3+}/\Sigma\text{Fe}$ ratio can be varied from 0 to 1.0. This in turn suggests that the Fe_4O_5 phase should be stable over a wide range of oxygen fugacities, making it more likely to be present in the deepest part of the upper mantle and transition zone.

A variety of M_4O_5 phases with the CaFe_3O_5 -type structure can be considered as essentially new additions to the phase relations of several simple oxide systems at the high-pressure and temperature conditions at which the spinel-structured phase becomes unstable in the same systems. It is to be expected that these phases can also form complex solid solutions analogous to those observed for spinels. Furthermore, our results indicate that, like spinel (e.g., O'Neill and Navrotsky 1983), cation order-disorder phenomena may help to stabilize the M_4O_5 phase, particularly at higher temperatures.

ACKNOWLEDGMENTS

This project was supported by grants from the Deutsche Forschungsgemeinschaft (DFG) to A.B.W. (Wo 652/20-1) and T.B.B. (Bo 2550/7-1). D.J. Frost is thanked for logistical help and advice.

REFERENCES CITED

- Enomoto, A., Kojitani, H., Akaogi, M., and Yusa, H. (2009) High-pressure transitions in MgAl_2O_4 and a new high-pressure phase of $\text{Mg}_2\text{Al}_2\text{O}_5$. *Journal of Solid State Chemistry*, 182, 389–395.
- Evrard, O., Malaman, B., Jeannot, F., Courtois, A., Alebouyeh, H., and Gerardin, R. (1980) Mise en évidence de CaFe_2O_6 et détermination des structures cristallines des ferrites de calcium $\text{CaFe}_{2+n}\text{O}_{4+n}$ ($n = 1, 2, 3$): nouvel exemple d'intercroissance. *Journal of Solid State Chemistry*, 35, 112–119.
- Farrugia, L.J. (1999) *WinGX* suite for small-molecule single-crystal crystallography. *Journal of Applied Crystallography*, 32, 837–838.
- Gerardin, R., Millon, E., Brice, J.F., Evrard, O., and Le Caer, G. (1985) Transfert électronique d'intervalence entre sites inéquivalents: étude de CaFe_3O_5 par spectrométrie Mössbauer. *Journal of Physics and Chemistry of Solids*, 46, 1163–1171.
- Guignard, J., and Crichton, W.A. (2014) Synthesis and recovery of bulk Fe_4O_5 from magnetite, Fe_3O_4 . A member of a self-similar series of structures for the lower mantle and transition zone. *Mineralogical Magazine*, 78, 361–371.
- Ibers, J.A., and Hamilton, W.C., Eds. (1974) *International Tables for X-ray Crystallography*, vol. IV, 366 p. Kynoch, Dordrecht, The Netherlands.
- Ishii, T., Kojitani, H., Tsukamoto, S., Fujino, K., Mori, D., Inaguma, Y., Tsujino, N., Yoshino, T., Yamazaki, D., Higo, Y., Funakoshi, K., and Akaogi, M. (2014) High-pressure phase transitions in FeCr_2O_4 and structure analysis of new post-spinel FeCr_2O_4 and $\text{Fe}_2\text{Cr}_2\text{O}_5$ phases with meteoritical and petrological implications. *American Mineralogist*, 99, 1788–1797.
- Keppler, H., and Frost, D.J. (2005) Introduction to minerals under extreme conditions. In R. Miletich, Ed., *Mineral Behaviour at Extreme Conditions*. EMU Notes in Mineralogy, 7, 1–30.
- Lavina, B., Dera, P., Kim, E., Meng, Y., Downs, R.T., Weck, P.F., Sutton, S.R., and Zhao, Y. (2011) Discovery of the recoverable high-pressure iron oxide Fe_4O_5 . *Proceedings of the National Academy of Sciences*, 108, 17281–17285.
- Levy, D., Diella, V., Dapiaggi, M., Sani, A., Gemmi, M., and Pavese, A. (2004) Equation of state, structural behaviour and phase diagram of synthetic $\text{Mg-Fe}_2\text{O}_4$, as a function of pressure and temperature. *Physics and Chemistry of Minerals*, 31, 122–129.
- O'Neill, H.St.C., and Navrotsky, A. (1983) Simple spinels: crystallographic parameters, cation radii, lattice energies, and cation distribution. *American Mineralogist*, 68, 181–194.
- O'Neill, H.St.C., Annersten, H., and Virgo, D. (1992) The temperature-dependence of the cation distribution in magnesioferrite (MgFe_2O_4) from powder XRD structural refinements and Mössbauer spectroscopy. *American Mineralogist*, 77, 725–740.
- Oxford Diffraction (2006) Xcalibur CCD system, CrysAlis Software system, ver. 171.32.29. Oxford Diffraction, U.K.
- Robinson, K., Gibbs, G.V., and Ribbe, P.H. (1971) Quadratic elongation: a quantitative measure of distortion in coordination polyhedra. *Science*, 172, 567–570.
- Sheldrick, G.M. (2008) A short history of SHELX. *Acta Crystallographica A*, 64, 112–122.
- Trots, D.M., Kurnosov, A., Woodland, A.B., and Frost, D.J. (2012) The thermal breakdown of Fe_4O_5 at ambient pressure. *European Mineralogical Conference*, vol. 1, EMC2012-556-1.
- Uenver-Thiele, L., Woodland, A.B., Boffa Ballaran, T., and Frost, D.J. (2014) Stability and structure of $\text{Mg}_2\text{Fe}_2\text{O}_5$ at high P-T conditions. *Deutsche Mineralogische Gesellschaft Annual Meeting*, Jena (abs).
- Woodland, A.B., Frost, D.J., Trots, D.M., Klimm, K., and Mezouar, M. (2012) In situ observation of the breakdown of magnetite (Fe_3O_4) to Fe_4O_5 and hematite at high pressures and temperatures. *American Mineralogist*, 97, 1808–1811.
- Woodland, A.B., Schollenbruch, K., Koch, M., Boffa Ballaran, T., Angel, R.J., and Frost, D.J. (2013) Fe_4O_5 and its solid solutions in several simple systems. *Contributions to Mineralogy and Petrology*, 166, 1677–1686.

MANUSCRIPT RECEIVED JULY 22, 2014

MANUSCRIPT ACCEPTED SEPTEMBER 4, 2014

MANUSCRIPT HANDLED BY IAN SWAINSON